Supplementary Information

Table S1 Selected bond lengths (Å) and bond angles (°) of Cu(II) centers in **1** and **2**

Bond distances of **1** (in Å)		Bond angles of **1** (in Degree)	
Cu1–O1	1.891(2)	O1–Cu1–O1#1	70.00(2)
Cu1–O1#1	1.891(2)	O1–Cu1–N1#1	92.09(1)
Cu1–N1#1	1.924(3)	N1#1–Cu1–O1#1	88.28(1)
Cu1–N1	1.924(3)	O1–Cu1–N1	88.28(1)
Cu1–N2#1	1.936(3)	N1–Cu1–O1#1	92.09(1)
Cu1–N2	1.936(3)	N1–Cu1–N1#1	179.54(2)
		O1–Cu1–N2#1	167.80(1)
		N2#1–Cu1–O1#1	98.53(1)
		N1#1–Cu1–N2#1	83.19(1)
		N1–Cu1–N2#1	96.50(1)
		O1–Cu1–N2	98.53(1)
		N2–Cu1–O1#1	167.80(1)
		N2–Cu1–N1#1	96.50(1)
		N1–Cu1–N2	83.18(1)
		N2–Cu1–N2#1	93.19(2)
Bond distances of **2** (in Å)		Bond angles of **2** (in Degree)	
Cu1–N3	1.988(2)	N3–Cu1–N1	170.03(9)
Cu1–N1	2.018(2)	N3–Cu1–N2	89.99(9)
Cu1–N2	2.108(2)	N1–Cu1–N2	80.06(9)
Cu1–Cl2	2.299(8)	N3–Cu1–Cl2	93.34(7)
Cu1–Cl1	2.434(7)	N1–Cu1–Cl2	94.36(7)
		N2–Cu1–Cl2	144.20(7)
		N3–Cu1–Cl2	92.94(7)
		N1–Cu1–Cl1	90.59(7)
		N2–Cu1–Cl1	106.71(7)
		Cl2–Cu1–Cl1	108.69(3)

#1 -x+1, y, -z+1/2

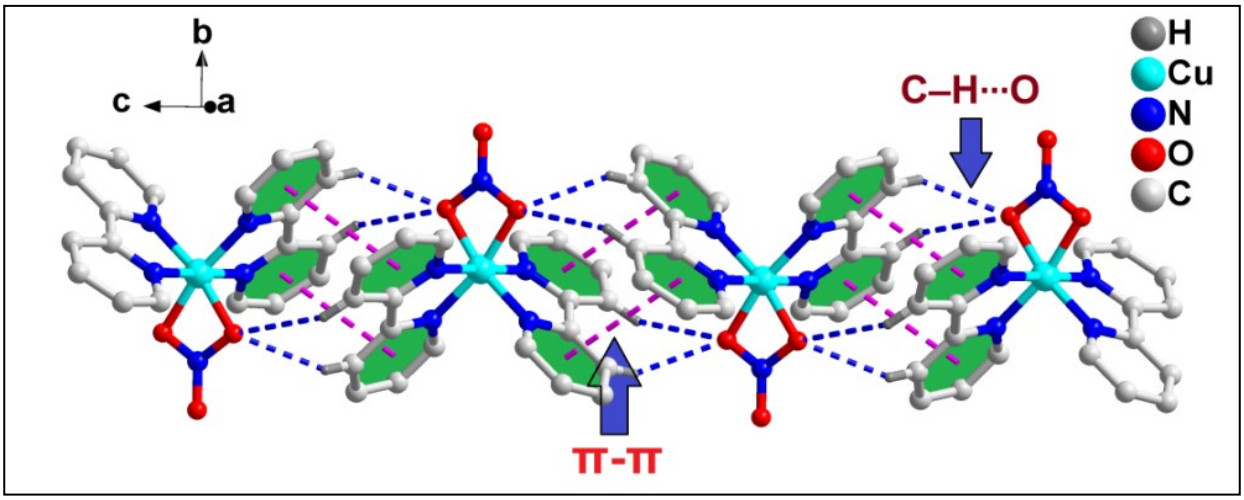

Fig. **S1** 1D supramolecular chain of **1** aided by π-stacking and C–H···O hydrogen bonding along crystallographic *c* axis.

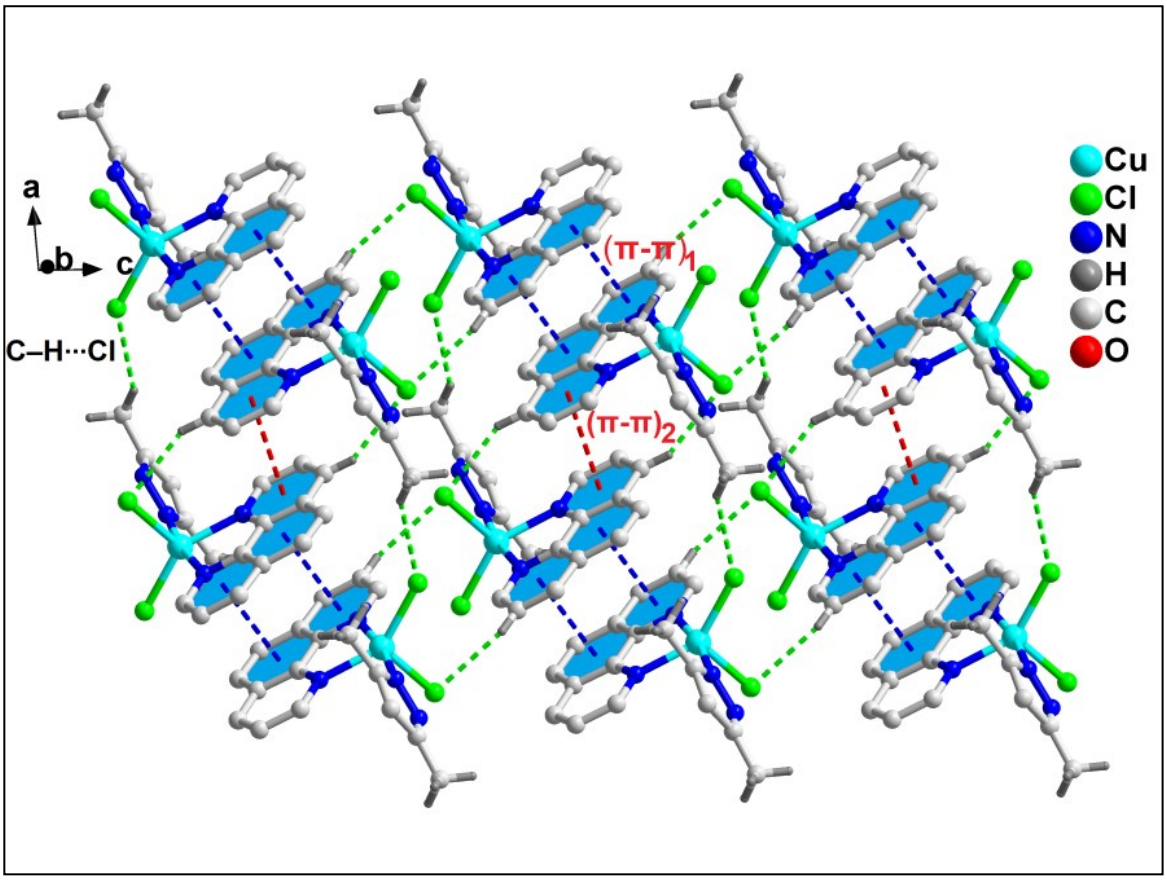

Fig. **S2** Layered assembly of compound **2** along the crystallographic *ac* plane.

Table S2 Selected Hydrogen bond distances (Å) and angles (°) for compounds **1** and **2**.

D–H···A	*d*(D–H)	*d*(D···A)	*d*(H···A)	<(DHA)
1				
C7–H7···O1	0.930(2)	3.270(5)	2.550(3)	134.4
C4–H4···O1	0.930(3)	3.636(5)	2.833(3)	145.2
O5–H5···O2	1.029(5)	3.170(4)	2.550(3)	148.0
O5–H5A···O4	0.989(5)	2.684(7)	1.912(5)	132.8
C1–H1···O3	0.929(4)	3.492(8)	2.694(7)	144.4
O6–H6B···O4	0.883(3)	2.768(6)	1.935(5)	156.1
2				
O1–H1B···Cl2	1.094(3)	3.325(3)	2.380(7)	146.3
O1–H1A···Cl1	0.970(3)	3.337(3)	2.406(8)	160.7
C8–H8···Cl1	0.950(3)	3.559(3)	2.684(7)	153.4
C2–H2···Cl1	0.950(3)	3.493(3)	2.776(7)	132.8
C9–H9···Cl2	0.949(3)	3.494(3)	2.778(8)	132.8
C17–H17···Cl1	0.980(4)	3.804(4)	2.938(8)	148.4
C3–H3···Cl2	0.950(3)	3.559(3)	2.683(8)	153.7
C15–H15···O1	0.950(3)	3.563(4)	2.743(3)	145.0
C9–H9···O1	0.949(3)	3.804(4)	2.991(4)	143.9
C14–H14A···Cl2	0.979(4)	3.640(4)	2.918(8)	131.4

S1 Spectral Studies

S1.1 FT-IR spectroscopy

The FT-IR spectra of the compounds **1** and **2** have been recorded in the region 4000-500 cm^{-1} (Fig. S3). Broad absorption peaks in the region 3200-3410 cm^{-1} in the spectra of the compounds can be attributed to the *ν*(O–H) stretching vibrations of the lattice water molecules.[1] The peaks at 1578 cm^{-1} due to the ν(C=N) stretching vibration of the *bpy* ring undergoes red shift to the lower frequency region in compound **1** indicating the coordination of N-atoms of *bpy* to the Cu(II) centre.[2] The absorption peaks observed at 777 and 1287 cm^{-1} can be correlated to the out of plane deformation and doubly degenerate stretching vibrations of the bidentate nitrate which confirms the coordination of nitrate ion at Cu(II) centre of **1**.[3] The strong absorption band at 1384 cm^{-1} for **1** indicates the presence of free nitrate anion.[4] The shifting of absorption peaks for *ν*(C–H) stretching vibrations of *phen* in **2**[5] corroborates that both the N-atoms of *phen* donates a pair of electron to the Cu(II) metal centre via coordinate covalent bonds. The bands around 1425 cm^{-1} and 1168 cm^{-1} can be assigned to the ring stretching vibrations [*ν*(C=C) and *ν*(C=N)] of *phen*.[6] The IR spectrum of **2** shows medium intensity peaks at around 3151 cm^{-1} that can be attributed to the *ν*(N–H) absorption of the mono-dentate *Hdmpz*.[7] Weak absorptions observed around 2970-2770 cm^{-1} can be attributed to the *ν*(C–H) vibration of the *Hdmpz* moieties.[8] The peaks at 1437, 1276 and 1168 cm^{-1} in **2** are due to ring stretching vibrations of *Hdmpz* rings (C–N, N–N and C=N respectively).[9]

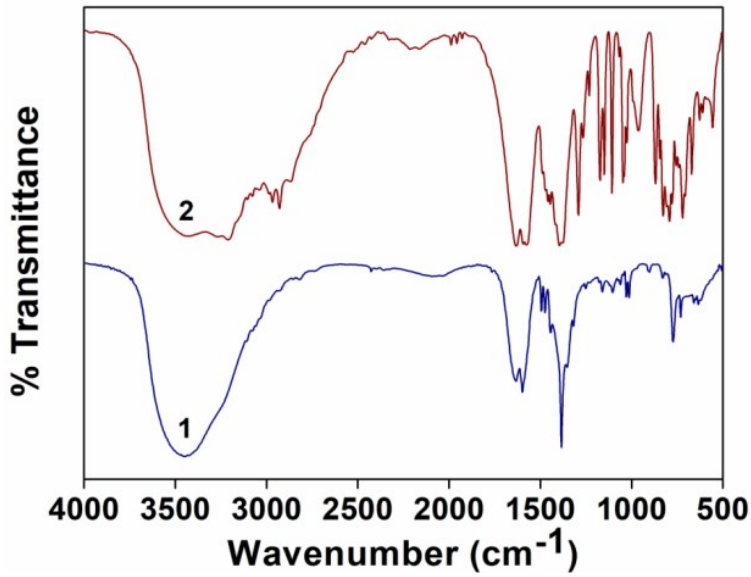

Fig. **S3** FT-IR spectra of the compounds **1** and **2**.

S1.2 Electronic spectroscopy

The electronic spectra of **1** have been recorded in solid phase as well as in aqueous phase. The solid-state UV-Vis-NIR spectrum of **1** (Fig. S4a) exhibits an intense peak at 269 nm assigned to π→π* transitions of the aromatic ligand.[10] The spectrum (Fig. S4a) shows broad absorptions at 681 nm resulting from the usual $^2E_g \rightarrow {}^2T_{2g}$ transition for Cu(II) complexes.[11] In the UV-Vis spectrum (Fig. S4b), the absorption peaks for π→π* and $^2E_g \rightarrow {}^2T_{2g}$ transitions are obtained at 276 and 661 nm respectively.[11]

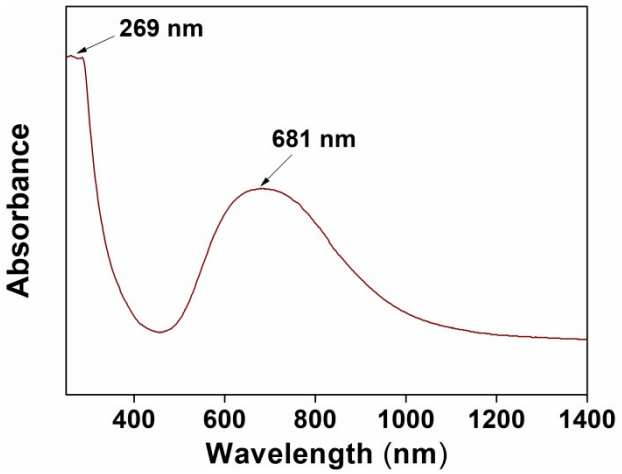

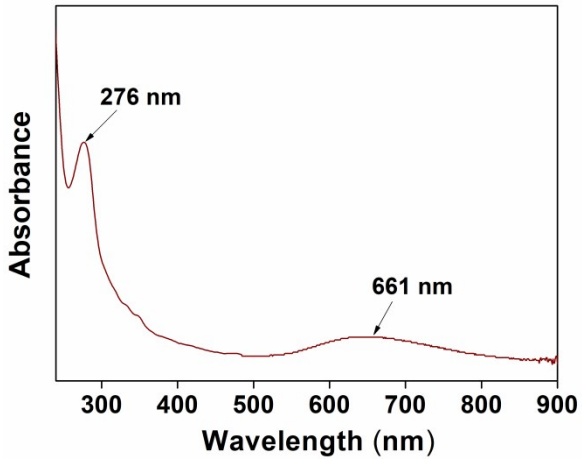

Fig. **S4**(**a**) UV-Vis-NIR spectrum of **1** (**b**) UV-Vis spectrum of **1**

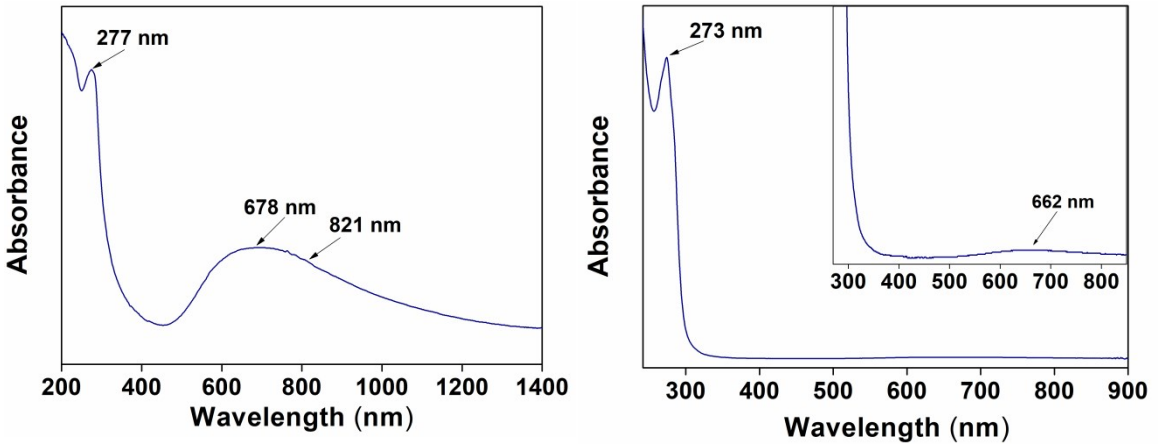

Fig. **S5**(**a**) UV-Vis-NIR spectrum of **2** (**b**) UV-Vis spectrum of **2**

The UV-Vis-NIR spectrum of **2** indicates the distortion of Cu(II) coordination in the complex from O_h symmetry (Fig. S5a). The broad band due to the d-d transition split into two, giving bands at 678 nm and 821 nm suggesting distorted square-pyramidal copper centre which agrees with the X-ray structure determination.[12] The UV-Vis spectrum (Fig. S5b) of **2** was also recorded in water. An octahedral and square pyramidal copper(II) complex is expected to show one broad absorption band in the electronic spectrum due to t_{2g} to e_g transition in the visible region. In **2**, absorption band was observed at 662 nm, is typical of those associated with d-d transitions in square pyramidal Cu^{2+} complexes.[13]

From the electronic spectra of **1** and **2** in both the solid and aqueous state, it can be observed that the electronic spectra in aqueous phase do not show marked differences from that of the respective solid-state spectra. So, it may be assumed that bonding modes as well as the geometries of the compounds do not undergo changes in the solution phase.[14]

S1.3 EPR spectral analysis

The x-band solid state EPR spectra of the compounds **1** and **2** were recorded at room temperature (Figs. S6 and S7). The spectrum of compound **1** shows an anisotropic signal characteristic of Cu(II) ion in octahedral geometry.[15] At room temperature, compound **1** exhibits an axial spectrum with $g_{\|} = 2.23$ and $g_{\perp} = 2.07$ without hyperfine splitting (Fig. S6). The fact that $g_{\|} > g_{\perp}$ is consistent with a d_{x2-y2} orbital ground state of the copper ion[16]; the spectrum is well consistent with a distorted octahedral geometry around the Cu(II) ion.[17]

The spectrum of compound **2** (Fig. S7) with $g_{\|} = 2.22$ and $g_{\perp} = 2.05$ is consistent with the square-pyramidal geometries found in the Cu(II) centers.[18] The spectral lines are broad and no hyperfine splitting was observed which may be attributed to the existence of spin exchange between the Cu(II) centers in the crystal structure. The observed $g_{\|} > g_{\perp}$ is consistent with a d_{x2-y2} orbital ground state of the copper ion and indicate distorted square-pyramidal geometry around penta-coordinated Cu(II) centers; thereby ruling out the possibility of trigonal bipyramidal geometry.[19] It has been well established that for coordination geometries corresponding to octahedron, square pyramid and square planar, the ground state is d_{x2-y2}.[20] The observed $g_{\|} > g_{\perp}$ values suggest the octahedral and square pyramidal geometries around the copper(II) centers in **1** and **2** respectively.[20]

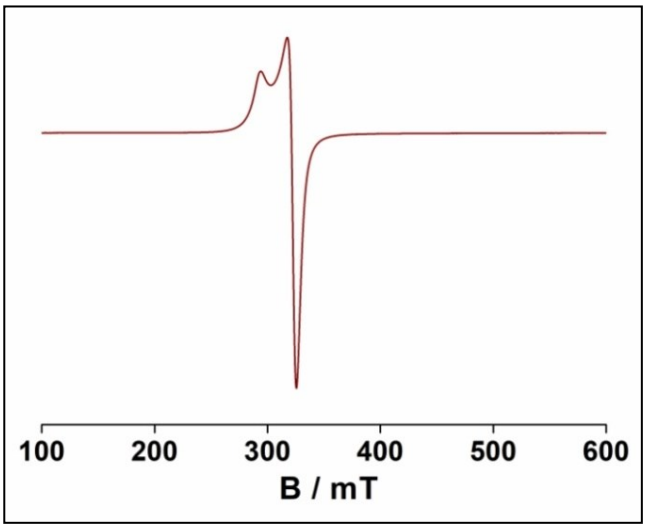

Fig. **S6** Room temperature EPR spectrum of crystalline sample of compound **1**.

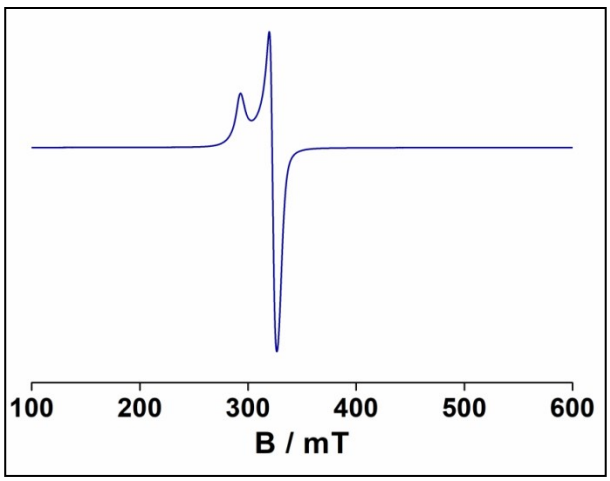

Fig. **S7** Room temperature EPR spectrum of crystalline sample of compound **2**.

S2 Thermal Analysis

Thermogravimetric curves of **1** and **2** were obtained in the temperature range of 25-700°C under N_2 atmosphere at the heating rate of 10°C/min (Fig. S8). For compound **1**, the 15.58% (calcd. 15.41%) decomposition in the temperature range 50-165°C is due to the loss of the five lattice water molecules[21] present in the compound. In the temperature range 170-330°C, the weight loss of about 19.35% (calcd. 21.16%) occurs due to the loss of lattice and coordinated nitrate moieties.[22] The weight loss of about 40.63% (calcd. 39.95%) over the temperature range of 330-600°C corresponds to the decomposition of 1.5 molecules of *bpy*.[23] For compound **2**, the 42.71% (calcd. 43.28%) weight loss in the temperature range 60-380°C is due to the loss of the one lattice water molecule[21], two coordinated chlorine[24] and one *Hdmpz*.[25] The weight loss of 18.20% (calcd. 20.15%) in the temperature range 380-450°C indicates the loss of 0.5 molecules of *phen*.[26]

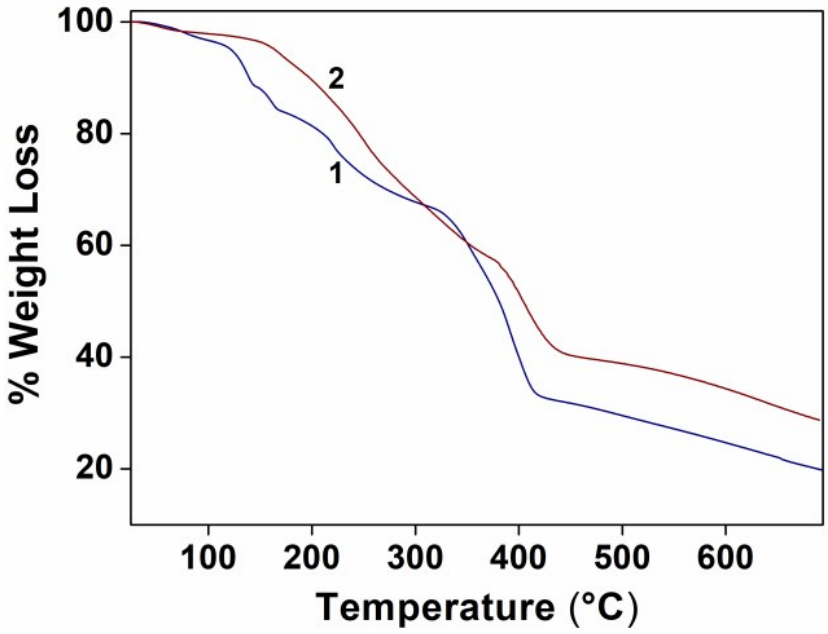

Fig. **S8** Thermogravimetric curves of compounds **1** and **2**.

Table S3 IC_{50} values of compounds **1** and **2** in DL Cell. IC_{50} values were determined using dose response curve. Significant cytotoxicity of *bipy*, *Hdmpz*, *phen*, $Cu(NO_3)_2 \cdot 3H_2O$ and $CuCl_2 \cdot 2H_2O$ in DL cells was not observed.

Sl. Nos.	Compounds	Cells	Tested duration	IC_{50} (μM)
1.	**1**	DL	24 hours	66.55
2.	**2**	DL	24 hours	135.33
3.	**1**	PBMC	24 hours	458.12
4.	**2**	PBMC	24 hours	645.33

Table S4 Intermolecular interactions between receptors and compounds **1** and **2**. The reference ligands were used from PDB entry file of respective receptor.

SI No	Receptors	Ligands	No. of H-bonds	Interactive amino acids	Binding score
1	BCL-2 (2O22)	Reference ligand	4	Gly142, Arg104, Thr93	-157.66
		Compound **1**	1	Gly142	-148.36
		Compound **2**	Nil	-	-
2	BCL-XL (2YXJ)	Reference ligand	4	Gly138, Glu129	-135.45
		Compound **1**	1	Glu129	-127.22
		Compound **2**	Nil	-	-

Supplementary References

1 (a) T. S. Mahapatra, A. Bauza, D. Dutta, S. Mishra, A. Frontera and D. Ray, *ChemistrySelect*, 2016, **1**, 64-75;

(b) O. Orhan, A. T. Colak, F. M. Emen, G. Kismali, O. Meral, T. Sel, G. K. Cilgi and M. Tas, *J. Coord. Chem*., 2015, **68**, 4003-4016;

(c) S. M. N. Islam, D. Dutta, A. K. Guha and M. K. Bhattacharyya, *J. Mol. Struct*., 2019, **1175**, 130-138.

2 E. Castellucci, L. Angeloni, N. Neto and G. Sbrana, *Chem. Phys*., 1979, **43**, 363-373.

3 Y. Li, X. Xu, R. Bian, K. Xie and Y. Zhang, *Inorg. Nano-Met. Chem*., 2020, **12**, 1842450-1842460.

4 (a) V. Y. Osipov, N. M. Romanov, F. M. Shakhov and K. Takai, *J. Opt. Technol*., 2018, **85**, 122-129.

(b) D. Dutta, S. Chetry, A. Gogoi, B. Choudhury, A. K. Guha and M. K. Bhattacharyya, *Polyhedron*, 2018, **151**, 381-393.

5 (a) Y. Prashanthi, K. Kiranmai and N. J. P. Subhashini, *Spectrochim. Acta*, 2008, **70**, 30-35;

(b) R. P. Sharma, A. Singh, P. Brandao, V. Felix and P. Venugopalan, *Inorg. Chem*., 2011, **376**, 64-72;

(c) P. Sharma, P. Sarma, A. Frontera, M. Barcelo-Oliver, A. K. Verma, B. Sarma, T. Barthakur and M. K. Bhattacharyya, *J. Mol. Struct*., 2020, **1229**, 129486-129502.

6 (a) H. H. Hammud, U. Kortz, S. Bhattacharya, S. Demirdjian, E. Hariri, S. Isber, E. S. Choi, B. Mirtamizdoust, M. Mroueh and C. F. Daher, *Inorg. Chim. Acta*, 2020, **506**, 119533;

(b) U. Saha, D. Dutta, A. Bauzá, A. Frontera, B. Sarma and M. K. Bhattacharyya, *Polyhedron*, 2019, **159**, 387-399.

7 (a) J. Li, Y. H. Xing, H. Y. Zhao, Z. P. Li, C. G. Wang, X. Q. Zeng, M. F. Ge and S. Y. Niu, *Inorg. Chim. Acta*, 2009, **362**, 2788-2795;

(b) A. Gogoi, S. M. N. Islam, A. Frontera and M. K. Bhattacharyya, *Inorg. Chim. Acta*, 2019, **484**, 133-141.

8 Y. Wang, X. M. Lin, F. Y. Bai and L. X. Sun, *J. Mol. Struct*., 2017, **1149**, 379-386.

9 A. Direm, M. Tursun, C. Parlak and N. B. Cherif, *J. Mol. Struct*., 2015, **1093**, 208-218.

10 C. Singh, S. Mukhopadhyay and S. K. Das, *Inorg. Chem*., 2018, **57**, 6479-6490.

11 (a) S. Choubey, S. Roy, K. Bhar, R. Ghosh, P. Mitra, C. Lin, J. Ribas and B. K. Ghosh, *Polyhedron*, 2013, **55**, 1-9;

(b) L. K. Das, S. W. Park, S. J. Cho and A. Ghosh, *Dalton Trans*., 2012, **41**, 11009-11017.

12 G. Sciortino, J. Maréchal, I. Fábián, N. Lihi and Eugenio Garribba, *J. Inorg. Biochem*., 2020, **204**, 110953-110963.

13 (a) M. K. Bhattacharyya, D. Dutta, S. M. N. Islam, A. Frontera, P. Sharma, A. K. Verma and A. Das, *Inorg. Chim. Acta*, 2020, **501**, 119233-119246;

(b) R. P. Sharma, A. Saini, S. Singh, P. Venugopalan and W. T. A. Harrison, *J. Fluorine Chem*., 2010, **131**, 456-460.

14 (a) M. Ghosh, A. Majee, M. Nethaji and T. Chattopadhyay, *Inorg. Chim. Acta*, 2009, **362**, 2052-2055;

(b) H. Nath, D. Dutta, P. Sharma, A. Frontera, A. K. Verma, M. Barceló-Oliver, M. Devi and M. K. Bhattacharyya, *Dalton Trans*., 2020, **49**, 9863-9881;

(c) C. Yenikaya, M. Poyraz, M. Sari, F. Demirci, H. Ilkimen and O. Buyukgungor, *Polyhedron*, 2009, **28**, 3526-3532.

15 M. K. Bhattacharyya, U. Saha, D. Dutta, A. Das, A. K. Verma and A. Frontera, *RSC Adv*., 2019, **9**, 16339-16356;

16 U. Saha, D. Dutta, H. Nath, A. Franconetti, A. Frontera and M. K. Bhattacharyya, *Inorg. Chim. Acta*, 2019, **488**, 159-169.

17 P. Mateus, R. Delgado, V. Andre and M. T. Duarte, *Inorg. Chem*., 2015, **54**(**1**), 229-240.

18 B. Annaraj, C. Balakrishnan and M. A. Neelakantan, *J. Photoch. Photobio. B*, 2016, **160**, 278-291.

19 A. E. M. Ramadan, S. Y. Shaban, M. M. Ibrahim, S. A. Sallam, F. I. El-Shami and S. Al-Juaid, *J. Mater. Sci*., 2020, **55**, 6457-6481.

20 S. Roy, P. Mitra and A. K. Patra, *Inorg. Chim Acta*, 2011, **370**, 247-253.

21 A. Gogoi, D. Dutta, A. K. Verma, H. Nath, A. Frontera, A. K. Guha and M. K. Bhattacharyya, *Polyhedron*, 2019, **168**, 113-126.

22 O. Carp, L. Patron, L. Diamandescu and A. Reller, *Thermochim. Acta*, 2002, **390**, 169-177.

23 D. Czakis-Sulikowska, A. Malinowska and J. Radwanska-Doczekalska, *Polish J. Chem*., 2000, **74**, 607-614.

24 Q. Yang, S. Chen and S. Gao, *J. Therm. Anal. Calorim*., 2007, **89**, 567-571.

25 P. M. Takahashi, A. V. G. Netto, A. E. Mauro and R. C. G. Frem, *J. Therm. Anal. Calorim*., 2005, **79**, 335-338.

26 Y. Qi, Y. Wang, C. Hu, M. Cao, L. Mao and E. Wang, *Inorg. Chem*., 2003, **42**, 8519-8523.